Journal of Solid State Chemistry **147,** 438–449 (1999)
Article ID jssc.1999.8358, available online at http://www.idealibrary.com on IDEAL®

New Compounds $In_3Ti_2AO_{10}$, $In_6Ti_6BO_{22}$, and Their Solid Solutions (*A*: Al, Cr, Mn, Fe, or Ga; *B*: Mg, Mn, Co, Ni, Cu, or Zn): Synthesis and Crystal Structures

Francisco Brown and Noboru Kimizuka[1]

Departamento de Investigaciones en Polimeros y Materiales, Universidad de Sonora, Hermosillo, Sonora, C.P. 83000 Mexico

Yuichi Michiue, Takahiko Mohri, and Masaki Nakamura

National Institute for Research in Inorganic Materials, 1-1 Namiki, Tsukuba-shi, Ibaraki-ken, 305-0044 Japan

and

Masahiro Orita and Kiyoshi Morita

Hoya R&D Center, Hoya Corporation, 3-1-1 Musashino, Akishima-shi, Tokyo, 196-8510 Japan

Received December 15, 1998; in revised form April 22, 1999; accepted May 7, 1999

New compounds, $In_3Ti_2AO_{10}$ (*A*: Al, Cr, Mn, Fe, or Ga) and $In_6Ti_6BO_{22}$ (*B*: Mg, Mn, Co, Ni, Cu, or Zn) were synthesized at and above 1000°C in air through solid-state reactions among the constituent cation oxide powders. They are isostructural with the monoclinic and/or orthorhombic $In_3Ti_2FeO_{10}$ having a pyrochlore-related crystal structure with a commensurate or incommensurate modulated structure. The high-temperature phase is orthorhombic, and the low-temperature phase is monoclinic. The lattice constants of $In_3Ti_2AO_{10}$ are as follows: $In_3Ti_2AlO_{10}$ (1200°C): a(Å) = 5.833(2), b(Å) = 3.371(2), and c(Å) = 12.060(6); $In_3Ti_2AlO_{10}$ (1100°C): a(Å) = 5.8368(7), b(Å) = 3.3721(4), c(Å) = 6.3402(8), and β(°) = 107.87(1); $In_3Ti_2CrO_{10}$ (1200°C): a(Å) = 5.9246(8), b(Å) = 3.3562(5), c(Å) = 6.3546(9), and β(°) = 108.10(1); $In_3Ti_2GaO_{10}$ (1200°C): a(Å) = 5.861(2), b(Å) = 3.385(1), and c(Å) = 12.094(4); $In_3Ti_2GaO_{10}$ (1000°C): a(Å) = 5.8742(9), b(Å) = 3.3828(5), c(Å) = 6.353(1), and β(°) = 107.87(1). $In_3Ti_2AlO_{10}$ and $In_3Ti_2GaO_{10}$ are polymorphic. The lattice constants of $In_6Ti_6BO_{22}$ are as follows: $In_6Ti_6MgO_{22}$ (1200°C): a(Å) = 5.9236(7), b(Å) = 3.3862(4), c(Å) = 6.3609(7), and β(°) = 108.15(1); $In_6Ti_6MnO_{22}$ (1200°C): a(Å) = 5.9361(9), b(Å) = 3.4031(5), c(Å) = 6.3435(10), and β(°) = 108.26(1); $In_6Ti_6CoO_{22}$ (1200°C): a(Å) = 5.9243(5), b(Å) = 3.3841(3), c(Å) = 6.3495(6), and β(°) = 108.18(1); $In_6Ti_6NiO_{22}$ (1200°C): a(Å) = 5.9191(6), b(Å) = 3.3729(3), c(Å) = 6.3568(6), and β(°) = 108.13(1); $In_6Ti_6CuO_{22}$ (1000°C): a(Å) = 5.916(2), b(Å) = 3.379(1), and c(Å) = 12.029(4); $In_6Ti_6ZnO_{22}$ (1200°C): a(Å) = 5.9223(6), b(Å) = 3.3830(3), c(Å) = 6.3576(6), and β(°) = 108.16(1). $In_6Ti_6BO_{22}$ (*B*: Mg, Mn, Co, Ni, or Zn) are monoclinic and $In_6Ti_6CuO_{22}$ is orthorhombic. Solid solutions were synthesized in between $In_3Ti_2AO_{10}$ (*A*: Al, Cr, Mn, Fe, or Ga) and $In_6Ti_6BO_{22}$ (*B*: Mg, Mn, Co, Ni, Cu or Zn), and their lattice constants were determined. Temperature in the parenthesis means synthesis temperature, and all the lattice constants were measured at room temperature. The relationship between the unit cells of $In_3Ti_2AO_{10}$, $In_6Ti_6BO_{22}$, their solid solutions, and the constituent cation elements of *A* and *B* are discussed in terms of their tendency for site preference. © 1999 Academic Press

Key Words: **$In_3Ti_2FeO_{10}$; $In_6Ti_6ZnO_{22}$; pyrochlore-type; incommensurate modulated structure; solid solution.**

INTRODUCTION

In_2O_3 is an important constituent compound for making transparent and electrically conductive materials at room temperature. Recently, it was reported that $MgIn_2O_4$ (1) having a spinel-type structure, $InGaMgO_4$ and $InGaZnO_4$ (2) having a layered $YbFe_2O_4$-type structure (3), and $GaInO_3$ in a thin film (4) are electrically conductive under low oxygen partial pressures. Edwards *et al.* established the phase relationships in the system In_2O_3–SnO_2–Ga_2O_3 at 1250°C and obtained a new phase $Ga_{3-x}In_{5+x}Sn_2O_{16}$ ($0.2 \le x \le 1.6$) which is electrically conductive (5). In the course of the investigation of the systems In_2O_3–A_2O_3–BO (*A*: Fe, Ga, or Al, *B*: Zn, Cu, or Co) at elevated temperatures, we established the phase relationships in these systems and clarified the crystal structures of $(InAO_3)_n(BO)_m$ (m and

[1]To whom correspondence should be addressed. E-mail address: nkimizuk@guaymas.uson.mx. Mailing address: A.Postal 792, Hermosillo, Sonora, C.P. 83000 Mexico.

0022-4596/99 $30.00

n are natural numbers) having layered crystal structures (6–12). Thereafter, we started establishing the phase relationships in the system In_2O_3–TiO_2–Fe_2O_3 at 1100°C in air and obtained a new compound, $In_3Ti_2FeO_{10}$, (hereafter we define this phase as unison-X_1 after (13)), whose crystal structures are related closely to $R_2Ti_2O_7$ (R: rare earth element or Y) having a cubic pyrochlore-type crystal structure. The relationships between the lattice constants of $In_3Ti_2FeO_{10}$ and those of $R_2Ti_2O_7$ are approximately as follows:

(1) in the monoclinic phase (the lower temperature phase),

$$\mathbf{a}_m = (1/4) \times \mathbf{a}_p + (1/2) \times \mathbf{b}_p + (1/4) \times \mathbf{c}_p,$$

$$\mathbf{b}_m = (-1/4) \times \mathbf{a}_p + (0) \times \mathbf{b}_p + (1/4) \times \mathbf{c}_p,$$

$$\mathbf{c}_m = (1/4) \times \mathbf{a}_p + (-1/2) \times \mathbf{b}_p + (1/4) \times \mathbf{c}_p,$$

and

$$\beta(^\circ) = 109.47.$$

(2) in the orthorhombic phase (the higher temperature phase),

$$\mathbf{a}_o = (-1/4) \times \mathbf{a}_p + (-1/2) \times \mathbf{b}_p + (-1/4) \times \mathbf{c}_p,$$

$$\mathbf{b}_o = (-1/4) \times \mathbf{a}_p + (0) \times \mathbf{b}_p + (1/4) \times \mathbf{c}_p,$$

$$\mathbf{c}_o = (2/3) \times \mathbf{a}_p + (-2/3) \times \mathbf{b}_p + (2/3) \times \mathbf{c}_p,$$

where $\mathbf{a}_m$, $\mathbf{b}_m$, and $\mathbf{c}_m$ are the unit-cell vectors for the monoclinic system, $\mathbf{a}_o$, $\mathbf{b}_o$, and $\mathbf{c}_o$ are those for the orthorhombic system, and $\mathbf{a}_p$, $\mathbf{b}_p$, and $\mathbf{c}_p$ are those of the cubic pyrochlore-type structure. Roth (14) synthesized $R_2Ti_2O_7$ (R: Sm, Gd, Dy, Yb, or Y) at 1425–1550°C in air, and Brixner (15) did $R_2Ti_2O_7$ (R: Sm–Lu, Y, or Sc) having the pyrochlore-type structure at 1200–1350°C in air. In the $R_2Ti_2O_7$ the coordination number of R(III) is 8 and that of Ti(IV) is 6 (16). However, they did not report on $In_2Ti_2O_7$. $In_2Mn_2O_7$ having the cubic pyrochlore-type with a(Å) = 9.727(1) was synthesized under $P = 60$ kbar at $T = 850$°C by Raju *et al.* (17). Although the ionic radius of In(III) is located between those of Lu(III) and Sc(III) (18), In(III) takes the coordination number of 4, 5, 6, or 8 in oxide crystals. On the other hand, R (La–Lu, Y, or Sc) takes a coordination number of 6 and above. In the system In_2O_3–TiO_2 at 1000–1350°C in air, we did not obtain $In_2Ti_2O_7$ (13) which might have the pyrochlore-type structure, if it existed, as Roth thought previously. However, in the pseudoternary system In_2O_3–TiO_2–A_2O_3 (A: Al, Cr, Mn, Fe, or Ga) (Fig. 1) and the system In_2O_3–TiO_2–BO (B: Mg, Mn, Co, Ni, Cu, or Zn) (Fig. 2), we synthesized compounds which are isostructural with $In_3Ti_2FeO_{10}$ having the cubic pyrochlore-related structure. Conditions of syntheses of these compounds and their solid solutions in the powder states and the crystal structural properties investigated through X-ray single-crystal, powder diffractometry, and electron diffractometry are reported in the present paper. Each compound reported in the present paper contains In(III), and it may have properties such as transparency in the visible range and high electrical conductivity at room temperature, if it is reduced under lower oxygen partial pressures.

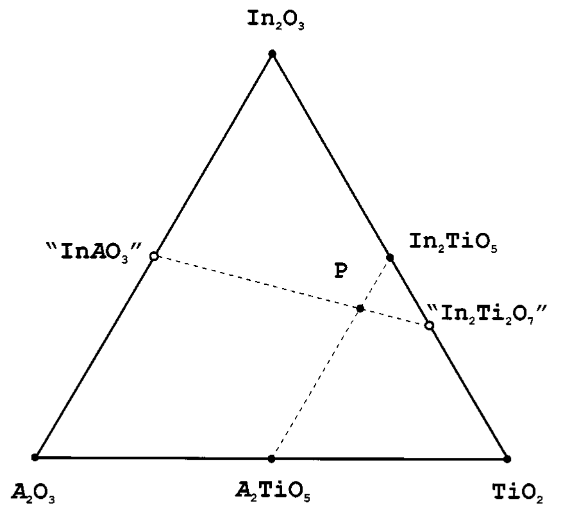

FIG. 1. $In_3Ti_2AO_{10}$ in the system In_2O_3–TiO_2–A_2O_3 (A: Al, Cr, Mn, Fe, or Ga). P: In_2O_3 : TiO_2 : A_2O_3 = 3 : 4 : 1 (in a mole ratio).

EXPERIMENTAL

Through solid-state reactions among oxide powders, we tried to synthesize multinary compounds in air at elevated temperatures. We used In_2O_3 (99.9%), TiO_2 (99.9%), A_2O_3

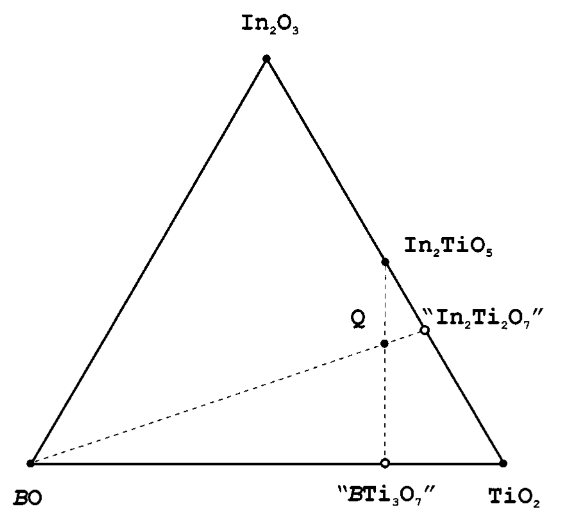

FIG. 2. $In_6Ti_6BO_{22}$ in the system In_2O_3–TiO_2–BO (B: Mg, Mn, Co, Ni, Cu, or Zn). Q: In_2O_3 : TiO_2 : BO = 3 : 6 : 1 (in a mole ratio).

(99.9%), and *B*O (99.9%) as the starting compounds. Prior to mixing them, we heated them at 850°C in air for 1 day. MnO was used as purchased. Mn_3O_4 was obtained by heating MnO at 1100°C in air for 5 days.

Synthesis of Powder Specimens

Calculated weights of In_2O_3, TiO_2, and A_2O_3; In_2O_3, TiO_2, and *B*O; or In_2O_3, TiO_2, A_2O_3, and *B*O (in a mole ratio) were weighed and mixed under ethanol in an agate mortar for about 25 min. Each mixture was pelletized (diameter: 12 mm; thickness: 2 mm) and heated in an alumina crucible in a box-type furnace with an Mo–Si alloy heating element for a fixed period and rapidly cooled at room temperature. At 1350°C mixtures were heated in sealed Pt tubes. The temperature fluctuation of the furnace was kept within ± 1°C. The weight of each specimen was carefully measured before and after heat treatment. Evaporation of the specimens was negligibly small. All of the specimens thus obtained were supplied for X-ray powder diffractometry (Cu$K\alpha$ radiation) with a graphite monochromator for phase identification and lattice constant measurement. Si powders (NBS standard reference number 640b, a(Å) = 5.4309) was used as the standard material for determining d-spacings. Calculation of lattice constants was made by the least square means method. Some of the specimens were supplied for electron diffractometry to observe the reciprocal lattice planes directly and to scanning electron microscopy to observe the surface states. Their data were consistent with the powder data.

Single-Crystal Growth of $In_3Ti_2FeO_{10}$

We heated a mixture of $In_2O_3:TiO_2:Fe_2O_3 = 3:4:1$ (in a mole ratio) at 1300°C in air for 1 day and obtained $In_3Ti_2FeO_{10}$ having an orthorhombic phase in a well-sintered polycrystalline state. It was carefully ground in an agate mortar and was charged into a Pt tube (diameter: 6 mm; height: 8 mm). It was reheated at 1680°C for 2 h and cooled to 1580°C at a cooling rate of 1°C/min. From 1580 to 1300°C it was cooled at a cooling rate of 5°C/min, followed by rapid cooling at room temperature. The crystals were annealed at 1200°C for 5 days. Plate-like single crystals with a maximum dimension of about 0.1 mm × 1 mm × 2 mm were obtained. A selected crystal was supplied for an automatic four circle goniometer to collect single-crystal data.

RESULTS AND DISCUSSION

[*I*] *Preparation of Specimens*

(a) $In_3Ti_2AO_{10}$ (*A*: Al, Cr, or Ga) and $In_6Ti_6BO_{22}$ (*B*: Mg, Mn, Co, Ni, Cu, or Zn): Mixtures of $In_2O_3:TiO_2:A_2O_3 = 3:4:1$ and $In_2O_3:TiO_2:BO = 3:6:1$ (in mole ratios) were heated in air at elevated temperatures. Weight gain was not observed in the heating process on the mixture of $In_2O_3:TiO_2:MnO = 3:6:1$ in air at 1200°C. We concluded that the oxidation state of manganese (II) did not change in the heating process for preparation. The detailed conditions for heating the mixtures are listed in Tables 1 and 2.

(b) Solid solutions of $In_3Ti_2AO_{10}$ (*A*: Al, Cr, Mn, Fe, or Ga) and $In_6Ti_6BO_{22}$: Mixtures of $In_2O_3:TiO_2:A_2O_3:BO = 6:10:1:1$ and $In_2O_3:TiO_2:Mn_3O_4 = 6:10:1$ (in mole ratios) were heated in air. Detailed conditions of syntheses are listed in Tables 3 and 4. Weight gain was not observed in the heating process of the mixture of $In_2O_3:TiO_2:Mn_3O_4 = 6:10:1$ between $T = 1100$ and 1250°C in air. We concluded that the oxidation state of manganese did not change in the heating process for preparation.

(c) Related compounds:

(1) We heated $In_2O_3:TiO_2:A_2O_3 = 4:4:2$ (in a mole ratio) (*A*: Al or Ga) and obtained a compound which is isostructural with $In_3Ti_2AO_{10}$. We concluded that $In_3Ti_2AO_{10}$ has a solid-solution range along the line "$InAO_3$"–"$In_2Ti_2O_7$" as in the system "$InFeO_3$"–"$In_2Ti_2O_7$" at 1100°C.

(2) We heated a mixture of $In_2O_3:TiO_2:SnO_2:Ga_2O_3:ZnO = 6:9:1:1:1$ (in a mole ratio) and obtained a

TABLE 1
$In_2O_3:TiO_2:A_2O_3 = 3:4:1$ (in a Mole Ratio) *A*: Al, Cr, Fe, or Ga

Compound	*T* (°C)	Heating period (day)		Lattice constants *a* (Å)	*b* (Å)	*c* (Å)	β (°)	*q*	*V* (Å³)	*a/b*	Color
$In_3Ti_2AlO_{10}$	1250	4 + 4 + 4	o	5.833(3)	3.3710(2)	12.060(6)		0.353	237.1	1.7303	Colorless
$In_3Ti_2AlO_{10}$	1100	3 + 3 + 5	m	5.8368(7)	3.3721(4)	6.3402(8)	107.87(1)	0.353	118.8	1.7309	Colorless
$In_3Ti_2CrO_{10}$	1200	2 + 2	m	5.9246(1)	3.3562(1)	6.3546(1)	108.10(1)	0.341	120.1	1.7653	Brown
$In_3Ti_2FeO_{10}$	1200	Ref. (13)	o	5.9089(5)	3.3679(3)	12.130(1)		0.333	241.4	1.7545	Brown
$In_3Ti_2FeO_{10}$	1100	Ref. (13)	m	5.9171(5)	3.3696(3)	6.3885(6)	108.02(1)	0.333	121.1	1.7560	Brown
$In_3Ti_2GaO_{10}$	1200	2 + 2	o	5.867(1)	3.3864(8)	12.084(3)		0.325	240.1	1.7324	Colorless
			h	3.3822(8)		12.088(3)			119.8		
$In_3Ti_2GaO_{10}$	1000	4 + 4 + 4	m	5.8742(9)	3.3828(5)	6.353(1)	107.87(1)	0.332	120.1	1.7365	Colorless

TABLE 2
$In_2O_3:TiO_2:BO = 3:6:1$ (in a Mole Ratio) *B*: Mg, Mn, Co, Ni, Cu, or Zn

Compound	*T* (°C)	Heating period (day)		Lattice constants *a* (Å)	*b* (Å)	*c* (Å)	β (°)	*q*	*V* (Å³)	*a*/*b*	Color
$In_6Ti_6MgO_{22}$	1200	1 + 3 + 3	m	5.9236(7)	3.3862(4)	6.3609(7)	108.15(1)	0.369	121.2	1.7493	Colorless
$In_6Ti_6MnO_{22}$	1200	2 + 2	m	5.9361(9)	3.4031(5)	6.3435(10)	108.26(1)	0.380	121.7	1.7443	Brown
$In_6Ti_6CoO_{22}$	1200	2 + 2	m	5.9243(6)	3.3841(3)	6.3495(6)	108.18(1)	0.375	120.9	1.7506	Brown
$In_6Ti_6NiO_{22}$	1200	3 + 3 + 3	m	5.9191(6)	3.3729(3)	6.3568(6)	108.13(1)	0.363	120.6	1.7547	Yellow/Brown
$In_6Ti_6CuO_{22}$	1000	1 + 1 + 2	o	5.916(2)	3.379(1)	12.031(4)		0.331	240.5	1.7510	Dark green
$In_6Ti_6ZnO_{22}$	1200	3 + 3	m	5.9223(6)	3.3830(3)	6.3576(6)	108.16(1)	0.360	121.0	1.7506	Colorless

monoclinic phase having larger lattice constants than $In_{12}Ti_{10}Ga_2ZnO_{42}$. All of the phases obtained and the conditions of syntheses are given in Tables 5 and 6.

All of the specimens prepared in the above conditions were in well-sintered polycrystalline states and were not electrically conductive at room temperature. The color of

TABLE 3
$In_2O_3:TiO_2:A_2O_3:BO = 6:10:1:1$ (in a Mole Ratio)

Compound	*T* (°C)	Heating period (day)		Lattice constants *a* (Å)	*b* (Å)	*c* (Å)	β (°)	*q*	*V* (Å³)	*a*/*b*	Color
				(a) $In_2O_3:TiO_2:Al_2O_3:BO = 6:10:1:1$							
$In_{12}Ti_{10}Al_2MgO_{42}$	1200	1 + 2 + 2	m	5.8795(6)	3.3602(4)	6.3466(7)	108.03(1)	0.355	119.2	1.7497	Colorless
$In_{12}Ti_{10}Al_2MnO_{42}$	1200	1 + 3	m	5.8850(7)	3.3689(4)	6.3399(8)	108.07(1)	0.359	119.5	1.7468	Brown
$In_{12}Ti_{10}Al_2CoO_{42}$	1200	1 + 3	m	5.8812(7)	3.3630(4)	6.3436(7)	108.07(1)	0.358	119.3	1.7488	Brown
$In_{12}Ti_{10}Al_2NiO_{42}$	1200	1 + 1 + 3	m	5.8786(6)	3.3590(4)	6.3439(7)	108.02(1)	0.356	119.1	1.7501	Yellowish brown
$In_{12}Ti_{10}Al_2CuO_{42}$	1100	2 + 2 + 3	o	5.876(1)	3.3769(8)	12.049(3)		0.356	239.0	1.7400	Yellowish green
$In_{12}Ti_{10}Al_2CuO_{42}$	1000	4 + 4 + 4	m	5.8758(8)	3.3656(5)	6.3375(9)	108.01(1)	0.354	119.2	1.7459	Yellowish green
$In_{12}Ti_{10}Al_2ZnO_{42}$	1200	1 + 2 + 2 + 3	m	5.8834(5)	3.3674(3)	6.3503(6)	108.04(1)	0.362	119.2	1.7472	Colorless
				(b) $In_2O_3:TiO_2:Cr_2O_3:BO = 6:10:1:1$							
$In_{12}Ti_{10}Cr_2MgO_{42}$	1200	1 + 2	m	5.9216(6)	3.3655(3)	6.3524(6)	108.10(1)	0.360	120.3	1.7595	Brown
$In_{12}Ti_{10}Cr_2MnO_{42}$	1200	1	m	5.9291(8)	3.3664(3)	6.3492(8)	108.16(1)	0.365	120.4	1.7613	Dark brown
$In_{12}Ti_{10}Cr_2CoO_{42}$	1200	1 + 2	m	5.9226(5)	3.3674(3)	6.3489(6)	108.13(1)	0.366	120.3	1.7588	Dark brown
$In_{12}Ti_{10}Cr_2NiO_{42}$	1200	1 + 1 + 2	m	5.9192(6)	3.3642(3)	6.3514(6)	108.11(1)	0.362	120.2	1.7596	Yellow/green
$In_{12}Ti_{10}Cr_2CuO_{42}$	1100	2 + 2	m	5.9266(5)	3.3726(3)	6.3436(5)	108.10(1)	0.366	120.5	1.7573	Dark brown
$In_{12}Ti_{10}Cr_2ZnO_{42}$	1200	1 + 3 + 3	m	5.9248(5)	3.3782(3)	6.3521(5)	108.12(1)	0.374	120.8	1.7538	Dark yellow
				(c) $In_2O_3:TiO_2:Fe_2O_3:BO = 6:10:1:1$							
$In_{12}Ti_{10}Fe_2MgO_{42}$	1200	2 + 1 + 2	m	5.9171(7)	3.3787(4)	6.3681(7)	108.10(1)	0.358	121.0	1.7513	Brown
$In_{12}Ti_{10}Fe_2MnO_{42}$	1200	1 + 2	m	5.9232(7)	3.3851(4)	6.3612(8)	108.13(1)	0.363	121.2	1.7498	Dark brown
$In_{12}Ti_{10}Fe_2CoO_{42}$	1200	1 + 2	m	5.9197(6)	3.3760(3)	6.3635(6)	108.10(1)	0.356	120.9	1.7535	Dark brown
$In_{12}Ti_{10}Fe_2NiO_{42}$	1200	1 + 2	m	5.9156(6)	3.3727(3)	6.3621(6)	108.09(1)	0.353	120.7	1.7540	Brown
$In_{12}Ti_{10}Fe_2CuO_{42}$	1100	2 + 2 + 3	m	5.9198(6)	3.3827(4)	6.3639(7)	108.15(1)	0.357	121.1	1.7500	Dark brown
$In_{12}Ti_{10}Fe_2ZnO_{42}$	1200	2 + 1 + 3	m	5.9180(6)	3.3772(3)	6.3556(6)	108.09(1)	0.356	120.9	1.7523	Brown
				(d) $In_2O_3:TiO_2:Ga_2O_3:BO = 6:10:1:1$							
$In_{12}Ti_{10}Ga_2MgO_{42}$	1250	3 + 4 + 4	o	5.8978(6)	3.3810(3)	12.079(1)		0.346	240.9	1.7444	Colorless
$In_{12}Ti_{10}Ga_2MgO_{42}$	1100	3 + 3 + 3	m	5.9051(6)	3.3777(3)	6.3596(6)	108.07(1)	0.346	120.6	1.7482	Colorless
$In_{12}Ti_{10}Ga_2MnO_{42}$	1300	4 + 4	o	5.9077(6)	3.3914(6)	12.065(1)		0.351	241.7	1.7419	Brown
$In_{12}Ti_{10}Ga_2MnO_{42}$	1100	3 + 3 + 3	m	5.9085(6)	3.3901(4)	6.3519(7)	108.11(1)	0.353	120.9	1.7429	Brown
$In_{12}Ti_{10}Ga_2CoO_{42}$	1300	4 + 4	o	5.900(1)	3.3823(6)	12.070(2)		0.346	240.9	1.7443	Yellow/brown
$In_{12}Ti_{10}Ga_2CoO_{42}$	1100	3 + 3 + 3	m	5.9046(6)	3.3794(3)	6.3573(6)	108.07(1)	0.348	120.6	1.7472	Yellow/brown
$In_{12}Ti_{10}Ga_2NiO_{42}$	1300	3 + 4 + 4	o	5.8996(9)	3.3812(5)	12.075(2)		0.340	240.9	1.7448	Yellow/brown
$In_{12}Ti_{10}Ga_2NiO_{42}$	1100	3 + 3 + 3	m	5.9034(6)	3.3760(3)	6.3591(9)	108.09(1)	0.347	120.5	1.7486	Yellow/brown
$In_{12}Ti_{10}Ga_2CuO_{42}$	1100	2 + 2 + 3 + 1	o	5.880(1)	3.3937(8)	12.085(3)		0.338	241.2	1.7326	Yellow/brown
			h	3.3943(7)		12.082(3)			120.6		
$In_{12}Ti_{10}Ga_2ZnO_{42}$	1250	3	o	5.8928(7)	3.3908(4)	12.076(1)		0.350	241.3	1.7379	Colorless
$In_{12}Ti_{10}Ga_2ZnO_{42}$	1100	3 + 3 + 3	m	5.9071(6)	3.3831(3)	6.3603(7)	108.07(1)	0.352	121.0	1.7460	Colorless

TABLE 4
$In_2O_3:TiO_2:Mn_3O_4 = 6:10:1$ (in a Mole Ratio)

Compound	T (°C)	Heating period (day)		Lattice constants a (Å)	b (Å)	c (Å)	β (°)	q	V (Å^3)	a/b	Color
$In_{12}Ti_{10}Mn_3O_{42}$	1250	3 + 3	o	5.529(1)	3.3916(7)	12.033(3)		0.344	241.9	1.7481	Brown
$In_{12}Ti_{10}Mn_3O_{42}$	1100	3 + 3 + 5	m	5.926(1)	3.3903(6)	6.332(1)	108.22(1)	0.344	120.8	1.7479	Brown

each specimen is shown in Tables 1–6. Although the monoclinic phases were directly formed from the starting mixtures, the orthorhombic phases were formed through the monoclinic phases as an intermediate state from the starting mixtures.

In Figs. 3–15, we show all of the phases prepared in the pseudobinary systems $In_6Ti_6BO_{22}$–$In_3Ti_2AO_{10}$ at elevated temperatures. Our conclusions from Figs. 3–15 are as follows: In the system $In_6Ti_6BO_{22}$–$In_3Ti_2AO_{10}$, a solid solution (1:2) is formed, which is isostructural with orthorhombic or monoclinic $In_3Ti_2FeO_{10}$. The orthorhombic phase is stable at higher temperature, and the monoclinic phase is stable at lower temperature. The phase transformation was reversible. However, the rate in the phase transformation from the orthorhombic to the monoclinic phase was slow, taking time on the order of days in the reaction period. We conclude that transformation may accompany the reconstructive process of the constituent ions in the crystalline states.

In the system In_2O_3–TiO_2–A_2O_3 (A: Al or Ga), there exist a solid solution having an orthorhombic system between $In_4Ti_2A_2O_{13}$ and $In_3Ti_2AO_{10}$ at 1200°C. Since their unit-cell volumes are nearly equal to each other, we conclude that the unit-cell volume is independent of the ratio of the cation to the anion from 8/13 to 6/10. This phenomenon was observed in the change of the lattice constants of the $In_3Ti_2FeO_{10}$ solid solution along the line between "$InFeO_3$"–"$In_2Ti_2O_7$" in the system In_2O_3–TiO_2–Fe_2O_3 at 1100°C (13). In_6Ti_6Mn(II)O_{22} and $In_{12}Ti_{10}A_2$Mn(II)O_{42} (A: Al, Cr, Fe, or Ga) and $In_{12}Ti_{10}$Mn(III)$_2$Mn(II)O_{42} are stable in air between 1100 and 1250°C.

[*II*] *Structural Study by X-Ray Single-Crystal and Powder Diffractometry*

(1) The single-crystal data for the orthorhombic $In_3Ti_2FeO_{10}$ are shown in Table 7 together with the powder data (13) which had been determined from both electron- and powder X-ray diffractometry. We conclude that the lattice constants and extinction rule determined from the powder data are consistent with those of the present single-crystal data.

(2) The crystal systems and their lattice constants for $In_3Ti_2AO_{10}$, $In_6Ti_6BO_{22}$, and $In_{12}Ti_{10}A_2BO_{42}$ are listed in Tables 1–6. From the similarity of their X-ray powder diffraction patterns to those of $In_3Ti_2FeO_{10}$ which has a phase transformation between the monoclinic and the orthorhombic phases between $T = 1100$–1200°C, we conclude that all of the phases shown in the present paper are isostructural with $In_3Ti_2FeO_{10}$. Figure 16 shows the dependence of the unit-cell symmetry of $In_3Ti_2AO_{10}$, $In_6Ti_6BO_{22}$, and $In_{12}Ti_{10}A_2BO_{42}$ upon the constituent cations A and B. From this figure, we conclude that

(3) $In_3Ti_2AO_{10}$ (A: Al or Ga) is polymorphic. The higher temperature form is orthorhombic, and the lower temperature form is monoclinic. $In_3Ti_2CrO_{10}$ is monoclinic at 1200 and 1300°C. $In_6Ti_6BO_{22}$ (B: Mg or Zn) has a monoclinic system at 1200 and 1350°C. $In_6Ti_6BO_{22}$ (B: Mn, Ni, or Co) has a monoclinic system at 1200°C. We did not obtain an orthorhombic phase in $In_6Ti_6BO_{22}$ (B: Mg, Mn, Co, Ni, or Zn). $In_6Ti_6CuO_{22}$ has an orthorhombic system at 1000 and 1100°C. The unit-cell volume changes (Å^3/molecular unit) accompanying the phase transformation from the

TABLE 5
$In_2O_3:TiO_2:A_2O_3 = 4:4:2$ (in a Mole Ratio) (A: Al or Ga)

Compound	T (°C)	Heating period (day)		Lattice constants a (Å)	b (Å)	c (Å)	β (°)	q	V (Å^3)	a/b	Color
$In_4Ti_2Al_2O_{13}$	1250	3 + 4 + 4	o	5.8359(9)	3.3698(5)	12.098(2)		0.270	237.9	1.7318	Colorless
			h	3.3692(6)		12.100(2)			119.0		
$In_4Ti_2Ga_2O_{13}$	1250	3 + 4 + 4	o	5.853(1)	3.3768(7)	12.104(3)		0.284	239.2	1.7333	Colorless
			h	3.383(1)		12.109(9)			120.0		

TABLE 6
$In_2O_3:TiO_2:SnO_2:Ga_2O_3:ZnO = 6:9:1:1:1$ (in a Mole Ratio)

Compound	T (°C)	Heating period (day)		Lattice constants				q	V (Å³)	a/b	Color
				a (Å)	b (Å)	c (Å)	β (°)				
$In_{12}Ti_9SnGa_2ZnO_{42}$	1200	2 + 2	m	5.918(1)	3.3949(7)	6.366(1)	108.04(1)	0.352	121.6	1.7432	Colorless

monoclinic to the orthorhombic phase are slightly negative except for $In_{12}Ti_{10}Mn_3O_{42}$ and $In_{12}Ti_{10}Al_2CuO_{42}$.

(4) The a/b is located between 1.765–1.730. Since the a/b of orthorhombic compounds such as $In_3Ti_2GaO_{10}$, $In_{12}Ti_{10}Ga_2CuO_{42}$, and $In_4Ti_2A_2O_{13}$ (A: Al or Ga) are nearly equal to $3^{1/2}$, we indexed the X-ray powder diffraction peaks as a hexagonal system for them. We show their lattice constants as a hexagonal system in Tables 1–6. In Figs. 17 and 18, we show the unit cells of the orthorhombic and the monoclinic phases. We recognize that a_m and a_o are nearly equal and b_m and b_o are also nearly equal to each other.

(5) The a/b in the orthorhombic phase is greater than or nearly equal to that of the monoclinic phase in the transformation.

(6) Since the unit-cell dimensions are actually determined by both In(III) and Ti(IV), being independent of the minor constituent cations of A and/or B, their differences are very small in $In_3Ti_2AO_{10}$, $In_6Ti_6BO_{22}$, and $In_{12}Ti_{10}A_2BO_{42}$, respectively. However, since the ionic radius of Ni(II) is the smallest among Mg(II), Mn(II), Co(II), Ni(II), Cu(II), and Zn(II) (18), it is reasonable that the volume of the unit cell of $In_{12}Ti_{10}A_2NiO_{42}$ (A: Al, Cr, Fe, or Ga) is smaller than the other compounds in Table 3.

All of the compounds in the present work have commensurate or incommensurate modulated diffraction spots along the b^* axis as $In_3Ti_2FeO_{10}$ does (13). Using hk_1lk_2 in which k_2 is an index for a periodicity of $q \times b^*$ in both the orthorhombic and the monoclinic phases, we indexed all of the X-ray powder diffraction peaks, and show q in Tables 1–6. We listed X-ray powder data for $In_6Ti_6ZnO_{22}$ and $In_{12}Ti_{10}Cr_2ZnO_{42}$ having a monoclinic system in Table 8 and $In_{12}Ti_{10}Ga_2MgO_{42}$ having an orthorhombic system in Table 9 as three examples in which the basic lattice constants were calculated from d-spacings of hk_10

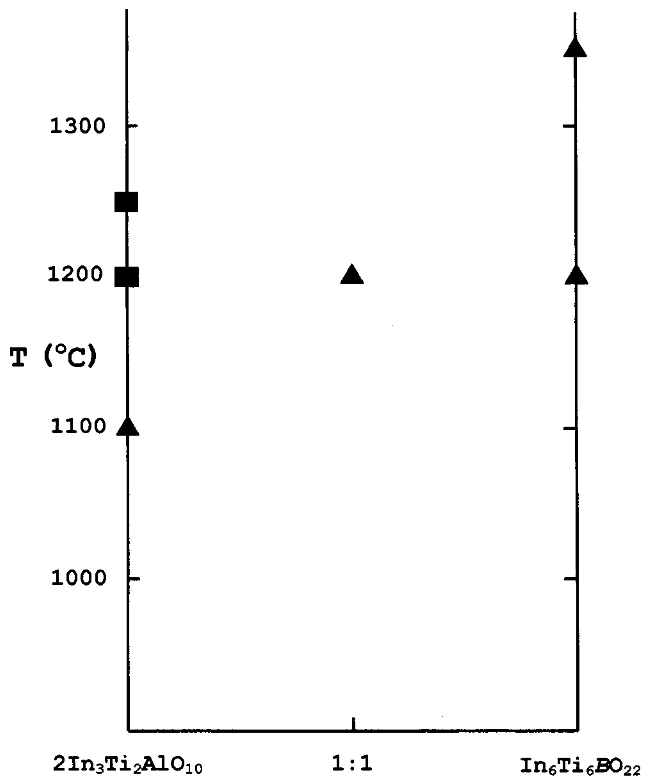

FIG. 3. The system $In_3Ti_2AlO_{10}$–$In_6Ti_6BO_{22}$ (B: Mg or Zn) in air.

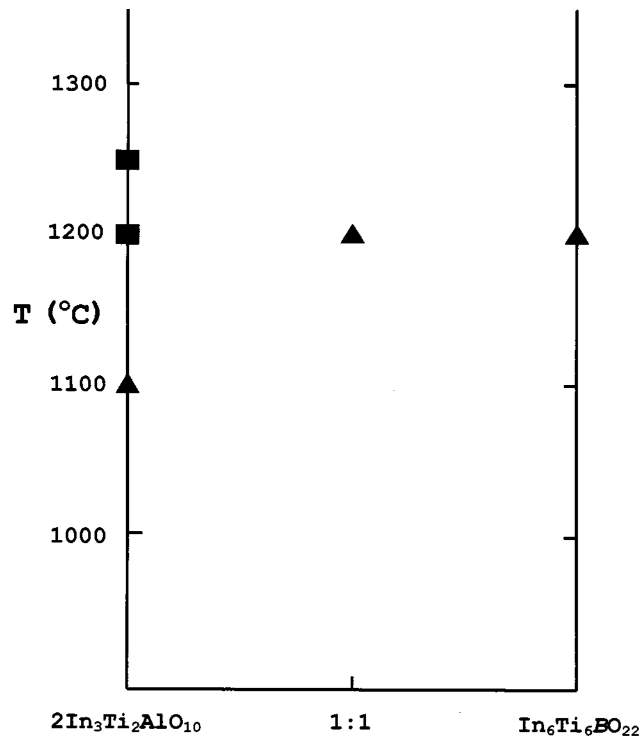

FIG. 4. The system $In_3Ti_2AlO_{10}$–$In_6Ti_6BO_{22}$ (B: Mn, Co, or Ni) in air.

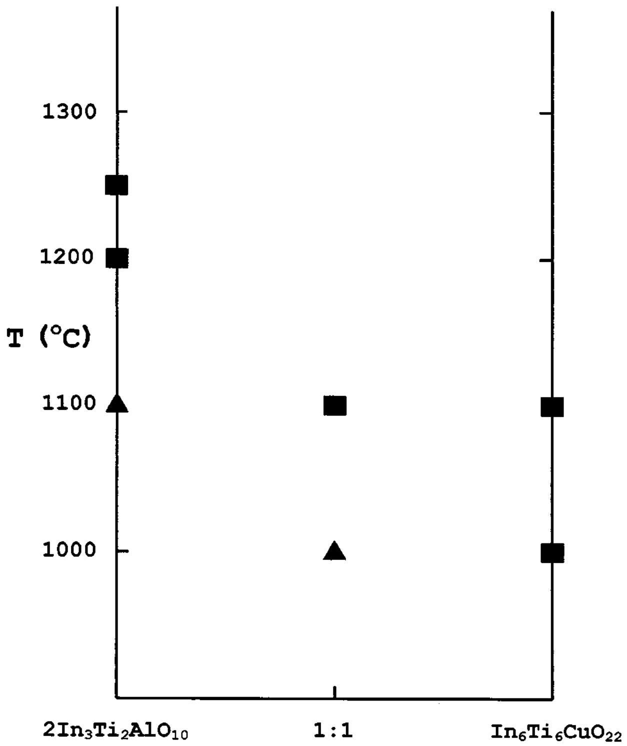

FIG. 5. The system $In_3Ti_2AlO_{10}$–$In_6Ti_6CuO_{22}$ in air.

using the least squares means method, and those of hk_1lk_2 (k_2 is equal to $+1$ or -1) were calculated from these basic lattice constants and q.

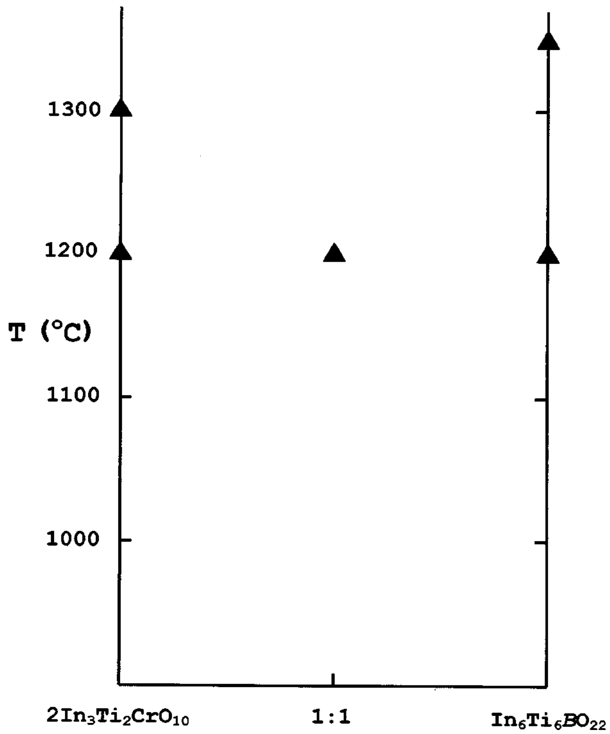

FIG. 6. The system $In_3Ti_2CrO_{10}$–$In_6Ti_6\mathit{B}O_{22}$ (*B*: Mg or Zn) in air.

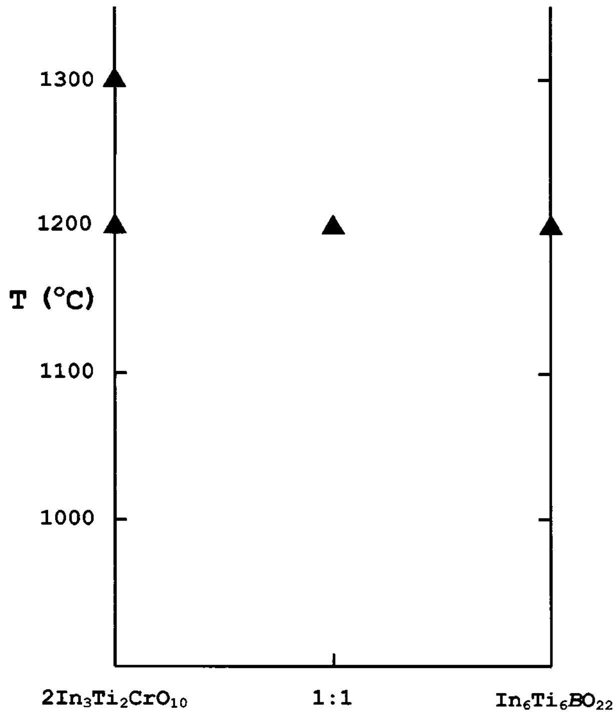

FIG. 7. The system $In_3Ti_2CrO_{10}$–$In_6Ti_6\mathit{B}O_{22}$ (*B*: Mn, Co or Ni) in air.

(7) In all of the compounds q is located between 0.270–0.380. $In_6Ti_6MnO_{22}$ has $q = 0.380$ and $In_{12}Ti_{10}Cr_2ZnO_{42}$ has $q = 0.374$, which are extraordinarily large. For

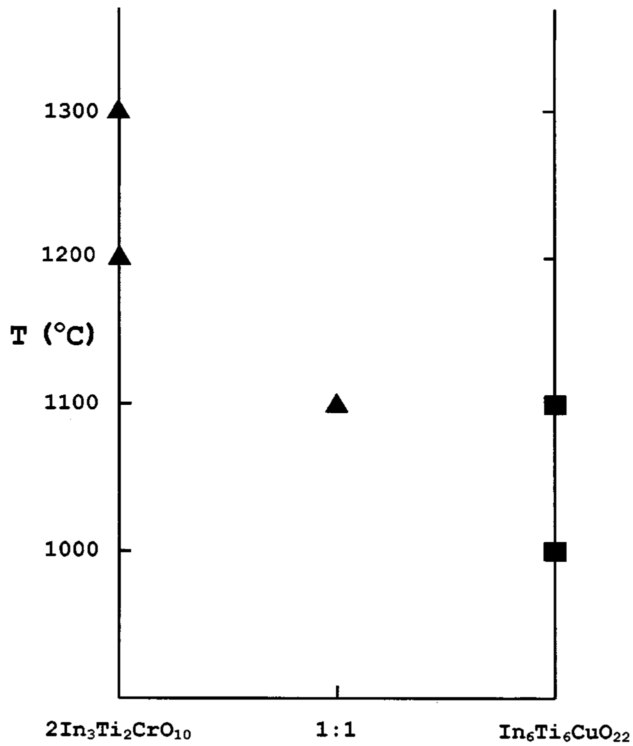

FIG. 8. The system $In_3Ti_2CrO_{10}$–$In_6Ti_6CuO_{22}$ in air.

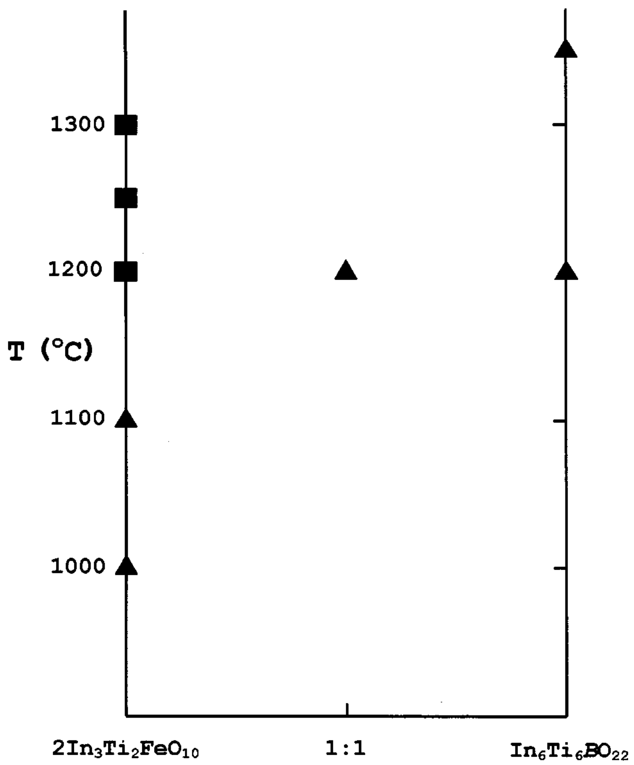

FIG. 9. The system $In_3Ti_2FeO_{10}$–$In_6Ti_6BO_{22}$ (B: Mg or Zn) in air.

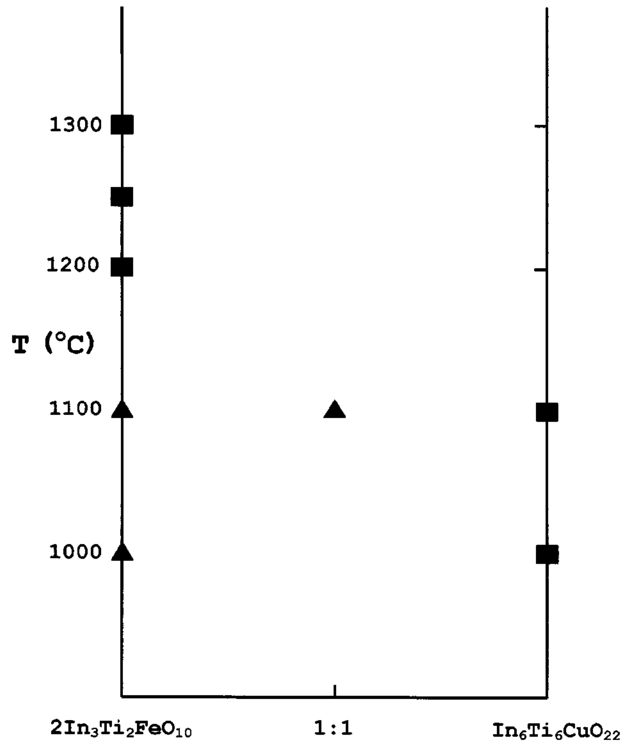

FIG. 11. The system $In_3Ti_2FeO_{10}$–$In_6Ti_6CuO_{22}$ in air.

many compounds q is located at 0.33–0.36. In the solid solution in the system $In_3Ti_2AO_{10}$–$In_6Ti_6BO_{22}$, q increases with the chemical composition change from $In_3Ti_2AO_{10}$ to $In_6Ti_6BO_{22}$ through $In_{12}Ti_{10}A_2BO_{42}$. This increment is seen in the $In_3Ti_2FeO_{10}$ solid solution in the system In_2O_3–TiO_2–Fe_2O_3 (13).

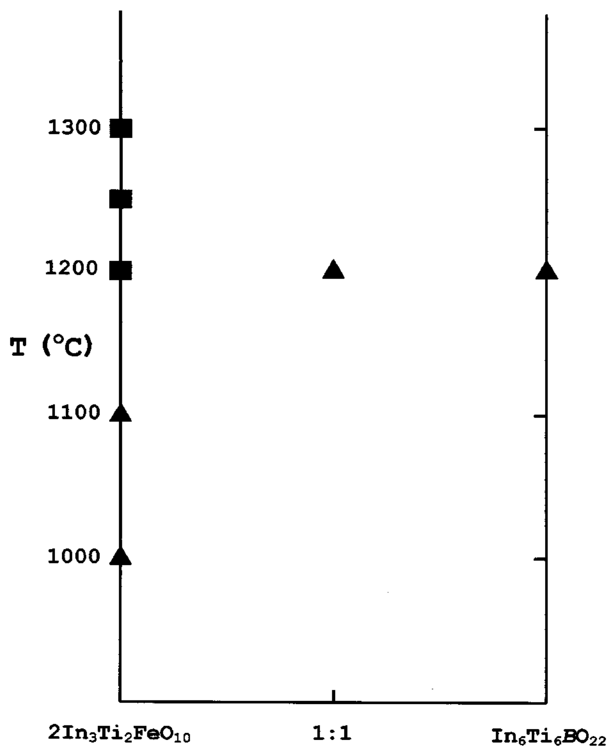

FIG. 10. The system $In_3Ti_2FeO_{10}$–$In_6Ti_6BO_{22}$ (B: Mn, Co, or Ni) in air.

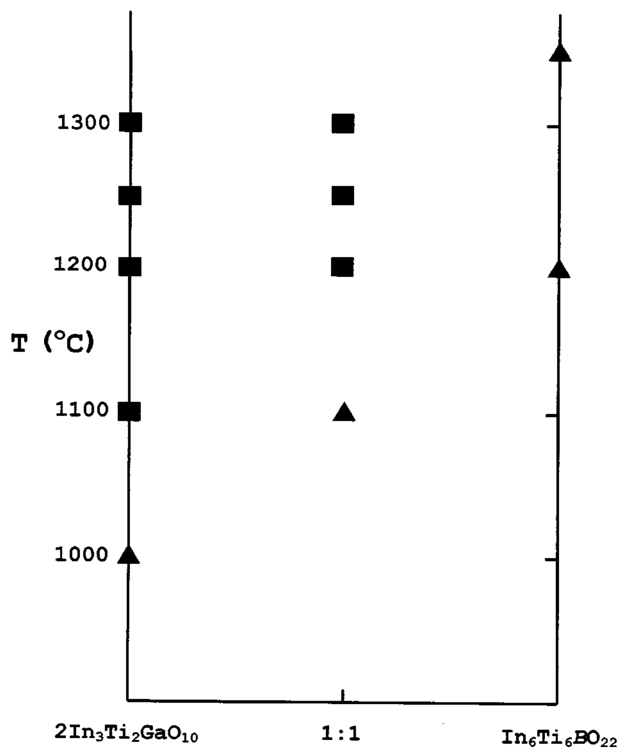

FIG. 12. The system $In_3Ti_2GaO_{10}$–$In_6Ti_6BO_{22}$ (B: Mg or Zn) in air.

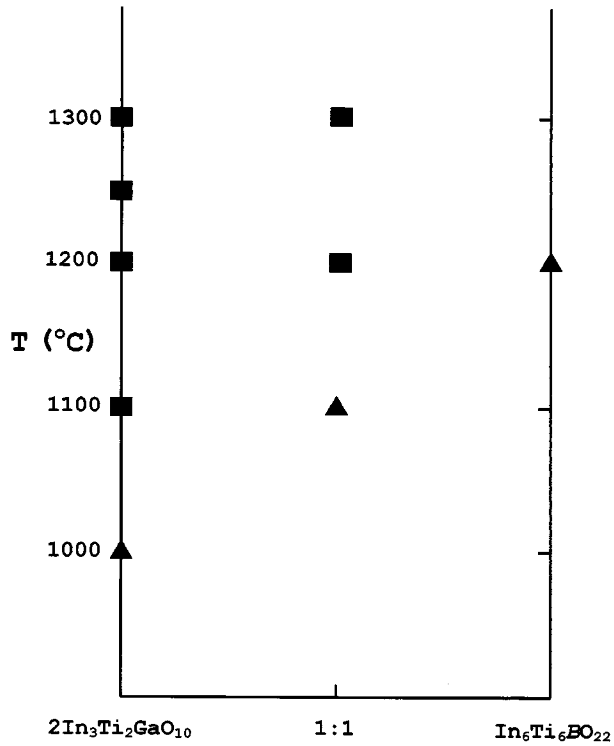

FIG. 13. The system $In_3Ti_2GaO_{10}$–$In_6Ti_6BO_{22}$ (B: Mn, Co, or Ni) in air.

(8) $In_{12}Ti_9SnGa_2ZnO_{42}$ was formed. A part of Ti(IV) in $In_{12}Ti_{10}Ga_2ZnO_{42}$ is replaced by Sn(IV) with a small increment in the lattice constants.

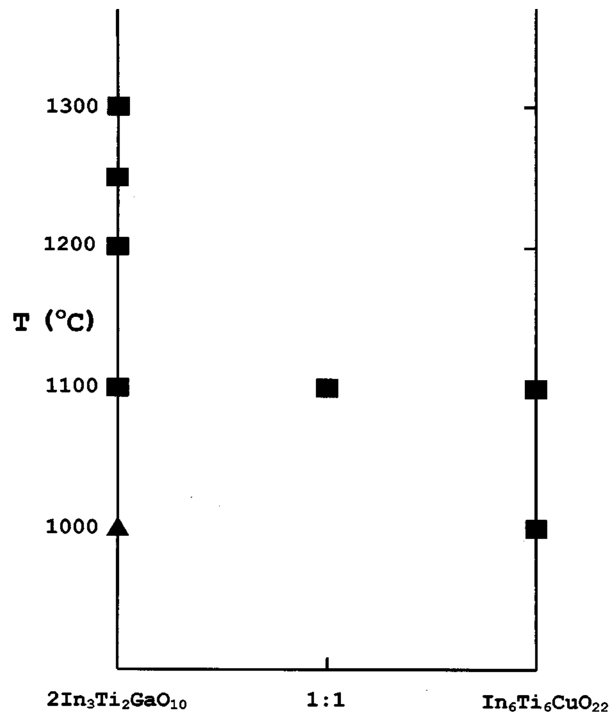

FIG. 14. The system $In_3Ti_2GaO_{10}$–$In_6Ti_6CuO_{22}$ in air.

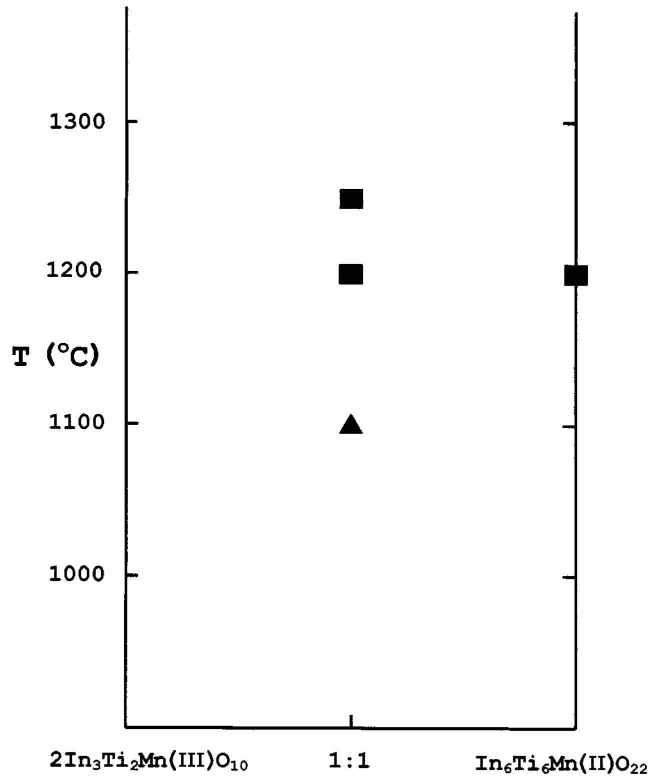

FIG. 15. The system In_3Ti_2Mn(III)O_{10}–In_6Ti_6Mn(II)O_{22} in air. (▲: compound having a monoclinic phase; ■: compound having an orthorhombic phase.

As we mentioned above, $In_2Ti_2O_7$ having the pyrochlore-type structure was not formed in the pseudobinary system In_2O_3–TiO_2 at elevated temperatures in air. However, we conclude that In_2O_3 and TiO_2 together with A_2O_3 and/or BO form compounds having a crystal structure which is related closely to the pyrochlore-type structure. We think it is important to recognize that as a member of A and B, Cr(III) has a strong tendency to take 6 CN and Ga(III) and Zn(II) to take 4 CN. The former makes a monoclinic phase.

TABLE 7
Crystal Data of $In_3Ti_2FeO_{10}$ (the High Temperature Form: Orthorhombic)

Crystal data	Single crystal data	Powder data (13)
a (Å)	5.834(1)	5.9089(5)
b (Å)	3.3505(9)	3.3679(3)
c (Å)	12.072(3)	12.130(1)
q	0.328	0.333 (=1/3)
V (Å^3)	236.4	241.4
Extinction law	$h + k_1 = 2n$ (hk_10)	$h + k_1 = 2n$ (hk_10)
	$k_1 = 2n$, $1 = 2n$ ($0k_110$)	$k_1 = 2n$, $1 = 2n$ ($0k_110$)
Space group	*Cmcm* (No. 63)	

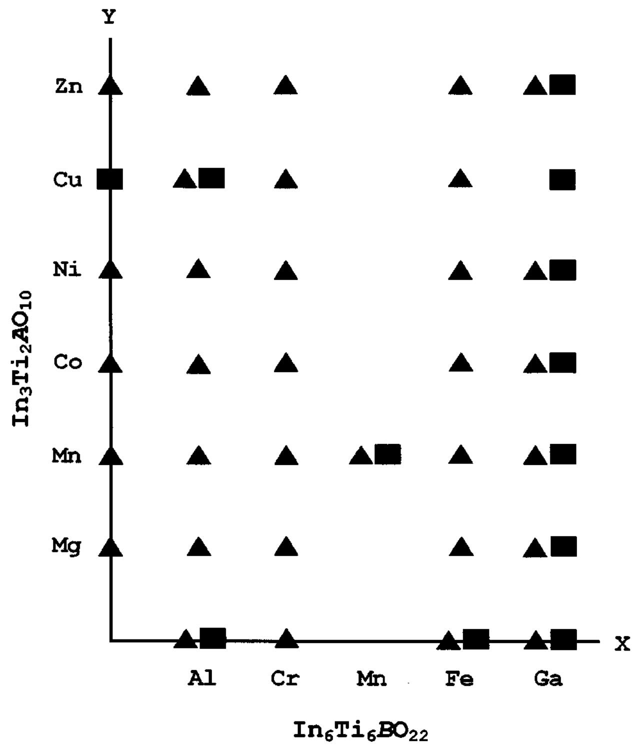

FIG. 16. The relationship between the unit-cell symmetry of the unison-X_1 and their constituent cations *A* (*A*: Al, Cr, Mn, Fe, or Ga) and *B* (*B*: Mg, Mn, Co, Ni, Cu, or Zn) The X axis means the $In_6Ti_6BO_{22}$, the Y axis means $In_3Ti_2AO_{10}$, and the X–Y plane means $In_{12}Ti_{10}A_2BO_{42}$. ▲: the monoclinic phase; ■: the orthorhombic phase.

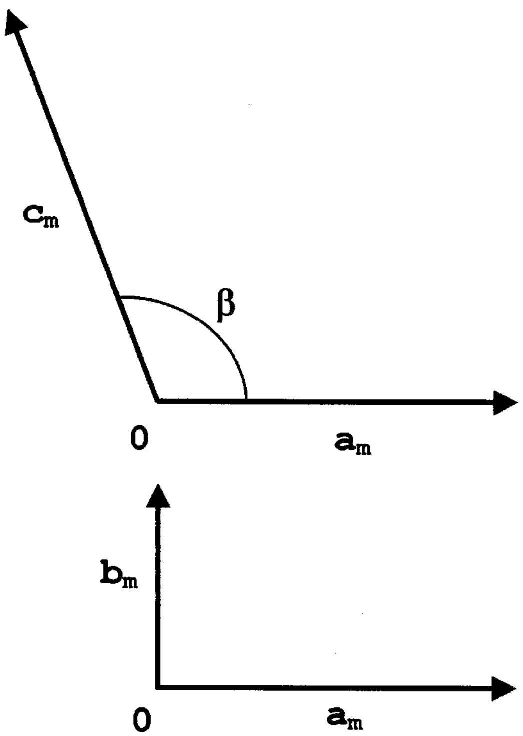

FIG. 17. The unit-cell vectors of the monoclinic phase: $\mathbf{a}_m$, $\mathbf{b}_m$, and $\mathbf{c}_m$ are the vectors of the monoclinic cell.

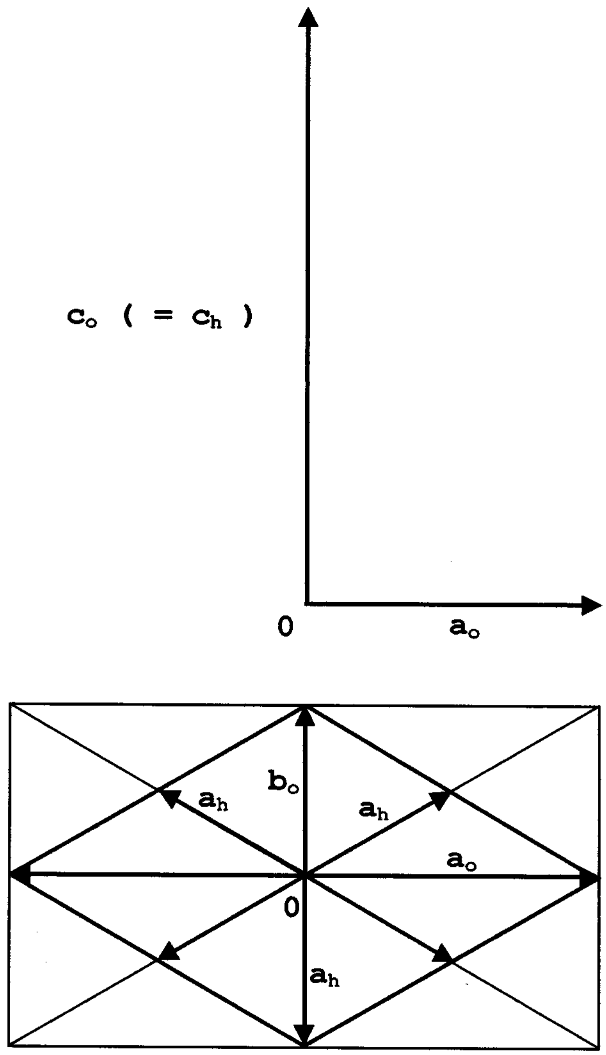

FIG. 18. The unit-cell vectors of the orthorhombic phase: $\mathbf{a}_o$, $\mathbf{b}_o$, and $\mathbf{c}_o$ are the vectors of the orthorhombic cell, and $\mathbf{a}_h$ and $\mathbf{c}_h$ are those of the hexagonal cell.

However, the latter has both orthorhombic and monoclinic phases.

The lattice constants of the present compounds are actually determined by both In(III) and Ti(IV). However, we consider that the unit-cell symmetry is determined by the minor constituent cations *A* and/or *B*.

(9) Preliminary single-crystal diffractometry for $In_3Ti_2FeO_{10}$ having an orthorhombic unit cell strongly suggests that it has a slightly deformed triangle lattice of oxygen ions (19). The thermal parameters of the oxygen ion are unusually large. An additional oxygen site is also found in a difference Fourier map. It can be speculated from these results that the displacive modulation of the oxygen ions is closely related to an observation of satellite reflections. The deviation from hexagonal to orthorhombic symmetry in

TABLE 8
X-Ray Powder data for $In_6Ti_6ZnO_{22}$ and $In_{12}Ti_{10}Cr_2ZnO_{42}$ Synthesized at 1200°C

				$In_6Ti_6ZnO_{22}$			$In_{12}Ti_{10}Cr_2ZnO_{42}$		
h	k_1	l	k_2	d_{obs} (Å)	d_{calc} (Å)	I (%)	d_{obs} (Å)	d_{calc} (Å)	I (%)
0	0	1	0	6.0352	6.0411	37	6.0352	6.0370	39
0	0	1	$\bar{1}$	5.167	5.082	2			
$\bar{1}$	1	1	$\bar{1}$	3.6266	3.6170	2	3.6471	3.6508	3
0	0	2	0	3.0188	3.0205	67	3.0168	3.0185	82
$\bar{2}$	0	1	0	2.9204	2.9229	7	2.9223	2.9236	7
$\bar{1}$	1	0	0	2.8964	2.8994	11	2.8964	2.8968	12
2	0	0	0	2.8128	2.8137	53	2.8146	2.8155	56
$\bar{1}$	1	1	0	2.7923	2.7948	100	2.7906	2.7918	100
2	0	0	1	2.6894	2.6917	2	2.6879	2.6880	2
$\bar{2}$	0	2	0	2.4789	2.4800	18	2.4789	2.4791	20
1	1	1	0	2.4619	2.4642	39	2.4606	2.4626	38
$\bar{2}$	0	2	1	2.3947	2.3958	2			
2	0	1	0	2.2925	2.2919	10	2.2936	2.2930	12
$\bar{1}$	1	2	0	2.2814	2.2828	24	2.2791	2.2803	26
$\bar{1}$	1	1	1	2.2136	2.2157	2	2.2033	2.2028	2
1	1	1	1	2.0375	2.0397	2	2.0297	2.0300	2
$\bar{2}$	0	3	0	1.9495	1.9502	5	1.9511	1.9488	3
1	1	2	0	1.9400	1.9418	7	1.9400	1.9407	8
$\bar{3}$	1	1	$\bar{1}$	1.8494	1.8514	2	1.8544	1.8546	4
2	0	2	0	1.7969	1.7983	15	1.7995	1.7987	12
$\bar{1}$	1	3	0	1.7942	1.7944	34	1.7916	1.7926	29
2	0	2	1				1.7632	1.7641	1
$\bar{3}$	1	1	0	1.7047	1.7050	24	1.7052	1.7050	25
0	2	0	0	1.6913	1.6915	12	1.6890	1.6891	13
$\bar{3}$	1	2	0	1.6405	1.6414	8	1.6405	1.6407	8
3	1	0	0		1.6405			1.6408	
0	2	1	0	1.6288	1.6289	3	1.6262	1.6266	4
$\bar{3}$	1	3	$\bar{1}$	1.5777	1.5793	2	1.5797	1.5803	3
3	1	1	1		1.5777				
$\bar{2}$	0	4	0	1.5469	1.5466	5	1.5460	1.5453	6
1	1	3	0	1.5418	1.5420	15	1.5409	1.5412	14
0	0	4	0	1.5099	1.5103	5	1.5090	1.5093	6
$\bar{3}$	1	3	0	1.4847	1.4854	14	1.4842	1.4846	19
3	1	1	0		1.4842			1.4844	
$\bar{4}$	0	1	0	1.4757	1.4755	8	1.4762	1.4763	5
0	2	2	0		1.4758		1.4741	1.4740	10
$\bar{2}$	2	1	0	1.4637	1.4640	2	1.4620	1.4625	6
$\bar{4}$	0	2	0	1.4616	1.4615	5		1.4618	
2	2	0	0	1.4498	1.4497	7	1.4486	1.4484	9
2	0	3	0	1.4382	1.4390	3			
$\bar{1}$	1	4	0	1.4370	1.4373	3	1.4354	1.4360	3
4	0	0	0				1.4077	1.4077	3
$\bar{2}$	2	2	0	1.3973	1.3974	5	1.3958	1.3959	6
$\bar{4}$	0	3	0	1.3706	1.3712	3	1.3713	1.3711	3
2	2	1	0	1.3605	1.3610	4	1.3598	1.3599	3
$\bar{3}$	1	4	0	1.3013	1.3019	1	1.3010	1.3009	2
3	1	2	0	1.3001	1.3006	1	1.3004	1.3008	2
$\bar{2}$	2	3	0	1.2777	1.2778	2	1.2763	1.2764	2
$\bar{2}$	0	5	0	1.2618	1.2619	1	1.2603	1.2608	2
1	1	4	0	1.2592	1.2592	3	1.2583	1.2585	2
$\bar{4}$	0	4	0	1.2400	1.2400	3	1.2394	1.2396	3
2	2	2	0	1.2321	1.2321	4	1.2313	1.2313	5
2	0	4	0	1.1850	1.1856	3	1.1855	1.1855	2
$\bar{1}$	1	5	0		1.1848		1.1835	1.1838	3
4	0	2	0	1.1458	1.1459	2	1.1462	1.1465	4
$\bar{2}$	2	4	0	1.1411	1.1414	4	1.1403	1.1401	4

TABLE 8—*Continued*

				$In_6Ti_6ZnO_{22}$			$In_{12}Ti_{10}Cr_2ZnO_{42}$		
h	k_1	l	k_2	d_{obs} (Å)	d_{calc} (Å)	I (%)	d_{obs} (Å)	d_{calc} (Å)	I (%)
$\bar{3}$	1	5	0	1.1306	1.1311	5	1.1302	1.1302	5
3	1	3	0	1.1302	1.1300	5		1.1300	
0	2	4	0	1.1270	1.1266	4	1.1251	1.1254	3
$\bar{5}$	1	2	0	1.1161	1.1159	1	1.1159	1.1161	1
$\bar{4}$	2	1	0	1.1118	1.1119	1	1.1116	1.1116	1
$\bar{5}$	1	1	0	1.1090	1.1094	2	1.1096	1.1097	3
$\bar{4}$	2	2	0	1.1058	1.1059	3	1.1052	1.1053	3
1	3	0	0		1.1057		1.1042	1.1042	2
$\bar{4}$	0	5	0	1.1022	1.1019	2	1.1016	1.1013	2
$\bar{1}$	3	1	0	1.0993	1.0996	2	1.0983	1.0981	3
2	2	3	0	1.0964	1.0960	1	1.0954	1.0954	2
$\bar{5}$	1	3	0	1.0855	1.0856	3	1.0857	1.0856	2
4	2	0	0	1.0817	1.0816	3	1.0810	1.0814	2
1	3	1	0	1.0762	1.0760	2	1.0747	1.0746	3
5	1	0	0	1.0682	1.0679	2	1.0686	1.0684	1
$\bar{4}$	2	3	0	1.0650	1.0652	3	1.0647	1.0645	3
$\bar{1}$	3	2	0	1.0592	1.0595	1	1.0578	1.0580	2
$\bar{2}$	0	6	0	1.0583	1.0583	1	1.0573	1.0574	2
1	1	5	0	1.0564	1.0567	3	1.0561	1.0561	3
$\bar{5}$	1	4	0	1.0268	1.0267	1	1.0260	1.0265	1
$\bar{2}$	2	5	0	1.0116	1.0114	2	1.0101	1.0104	1
0	0	6	0	1.0069	1.0068	2	1.0063	1.0062	2

$In_3Ti_2AO_{10}$ and $In_{12}Ti_{10}A_2BO_{42}$ becomes larger with A = Al, Ga, Fe, and Cr in this order. The crystal structural analysis for the compounds reported in the present article is in progress (19).

All of the X-ray powder data for the compounds synthesized in the present work will be reported to the International Centre for Diffraction Data.

TABLE 9
X-Ray Powder Data for $In_{12}Ti_{10}Ga_2MgO_{42}$ Synthesized at 1250°C

h	k_1	l	k_2	d_{obs} (Å)	d_{calc} (Å)	I (%)
0	0	2	0	6.0355	6.0395	50
1	1	1	$\bar{1}$	3.7010	3.7000	2
0	0	4	0	3.0170	3.0198	100
2	0	0	0	2.9488	2.9489	15
1	1	0	0	2.9300	2.9331	31
2	0	1	0	2.8640	2.8648	10
1	1	1	0	2.8480	2.8503	20
2	0	2	0	2.6509	2.6499	39
1	1	2	0	2.6373	2.6384	72
1	1	1	1	2.2670	2.2707	2
2	0	4	0	2.1090	2.1098	14
1	1	4	0	2.1034	2.1040	26
2	0	5	0	1.8681	1.8688	4
1	1	5	0	1.8630	1.8647	5
3	1	0	$\bar{1}$	1.8355	1.8373	2
3	1	0	0	1.6995	1.6995	26
0	2	0	0	1.6896	1.6904	12
3	1	1	0	1.6822	1.6829	2

TABLE 9—*Continued*

h	k_1	l	k_2	d_{obs} (Å)	d_{calc} (Å)	I (%)
2	0	6	0	1.6636	1.6627	8
1	1	6	0	1.6581	1.6598	16
3	1	2	0	1.6358	1.6360	8
0	2	2	0	1.6278	1.6279	4
3	1	4	$\bar{1}$	1.5694	1.5696	2
3	1	3	0	1.5676	1.5657	2
3	1	0	1	1.5469	1.5483	2
0	0	8	0	1.5100	1.5099	7
2	0	7	0	1.4899	1.4893	2
1	1	7	0	1.4873	1.4873	3
3	1	4	0	1.4809	1.4811	16
4	0	0	0	1.4754	1.4744	11
0	2	4	0		1.4751	
2	2	0	0	1.4658	1.4666	3
4	0	1	0	1.4642	1.4636	2
2	2	1	0	1.4551	1.4559	2
4	0	2	0	1.4328	1.4324	4
2	2	2	0	1.4246	1.4252	8
2	2	3	0	1.3767	1.3780	1
3	1	4	1	1.3766	1.3778	1
2	0	8	0	1.3429	1.3440	4
1	1	8	0		1.3425	
4	0	4	0	1.3245	1.3249	2
2	2	4	0	1.3193	1.3192	3
3	1	6	0	1.2977	1.2986	2
0	2	6	0	1.2949	1.2946	2
4	0	6	0	1.1899	1.1895	2
2	2	6	0	1.1853	1.1854	4
3	1	8	0	1.1288	1.1288	6
0	2	8	0	1.1261	1.1261	6
2	0	10	0	1.1174	1.1178	3
2	2	7	0		1.1175	
1	1	10	0	1.1171	1.1169	3
5	1	0	0	1.1137	1.1137	3
4	2	0	0	1.1111	1.1112	3
5	1	1	0	1.1094	1.1090	1
1	3	0	0	1.1072	1.1069	1
4	2	1	0	1.1060	1.1065	1
1	3	1	0	1.1027	1.1023	1
5	1	2	0	1.0953	1.0953	3
4	2	2	0	1.0928	1.0928	4
1	3	2	0	1.0889	1.0888	4
4	0	8	0	1.0548	1.0549	2
2	2	8	0	1.0524	1.0520	2
5	1	4	0	1.0451	1.0449	2
4	2	4	0	1.0424	1.0428	3
1	3	4	0	1.0394	1.0393	3
2	0	11	0	1.0289	1.0291	1
1	1	11	0	1.0283	1.0284	1
5	1	5	0	1.0115	1.0114	1
0	0	12	0	1.0070	1.0066	2
1	3	5	0	1.0064	1.0063	2

ACKNOWLEDGMENTS

One of the authors (N.K.) expresses his sincere thanks to Dr. M. Onoda and Dr. M. Saeki at NIRIM and Professor N. Ishizawa at the Tokyo Institute of Technology for their helpful discussions. A part of the present work was financially supported by the Japan International Cooperation Agency.

REFERENCES

1. N. Ueda, T. Omata, N. Hikuma, K. Ueda, H. Mizoguchi, T. Hashimota, and H. Kawazoe, *Appl. Phys. Lett.* **61,** 1954 (1992).
2. M. Orita, M. Takeuchi, H. Sakai, and H. Tanji, *Jpn, J. Appl. Phys.* **34,** L1550 (1995).
3. K. Kato, I. Kawada, N. Kimizuka, and T. Katsura, *Z. Kristallogr.* **141,** 314 (1975).
4. J. M. Phillips, J. Kwo, G. A. Thomas, S A. Carter, R. J. Cava, S. Y. Hou, J. J. Krajewski, J. H. Marshall, W. F. Peck, D. H. Rapkine, and R. B. van Dover, *Appl. Phys. Lett.* **65,** 115 (1994).
5. D. D. Edwards, T. O. Mason, F. Goutenoire, and K. R. Poeppelmeier, *Appl. Phys. Lett.* **70,** 1706 (1997).
6. N. Kimizuka and T. Takayama, *J. Solid State Chem.* **53,** 217 (1984).
7. M. Nakamura, N. Kimizuka, and T. Mohri, *J. Solid State Chem.* **86,** 16 (1990).
8. M. Nakamura, N. Kimizuka, and T. Mohri, *J. Solid State Chem.* **93,** 298 (1991).
9. M. Nakamura, N. Kimizuka, T. Mohri, and M. Isobe, *J. Solid State Chem.* **105,** 535 (1993).
10. N. Kimizuka, M. Isobe, M. Nakamura, and T. Mohri, *J. Solid State Chem.* **103,** 394 (1993).
11. N. Kimizuka, M. Isobe, and M. Nakamura, *J. Solid State Chem.* **116,** 170 (1995).
12. N. Kimizuka, E. Takayama-Muromachi, and K. Siratori, "Hand-Book on the Physics and Chemistry of Rare Earths," (K. A. Gschneidner, Jr. and LeRoy Eyring, Eds.), Vol. 13, Chapter 90, 283. North-Holland, Amsterdam, 1990.
13. F. Brown, M. J. R. Flores, N. Kimizuka, Y. Michiue, M. Onoda, T. Mohri, M. Nakamura, and N. Ishizawa, *J. Solid State Chem.* **144,** 91 (1999).
14. R. S. Roth, *J. Res. Nat. Bur. Stand.* **56,** 17 (1956).
15. L. H. Brixner, *Inorg. Chem.* **3,** 1065 (1964).
16. Knop, F. Brisse, L. Castelliz, and Sutarno, *Can. J. Chem.* **43,** 2812 (1965).
17. N. P. Raju, J. E. Greedan, and M. A. Subramanian, *Phys. Rev. B* **49,** 1086 (1994).
18. R. D. Shannon, *Acta Crystallogr. Sect. A* **32,** 279 (1976).
19. Y. Michiue, M. Watanabe, F. Brown, N. Kimizuka, M. Orita, and H. Ohta, *Acta Crystallogr. Sect. C*, in press.